CHALMERS

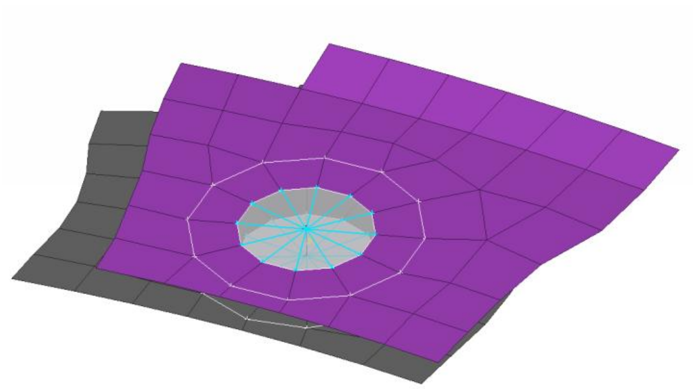

Fatigue Life and Stiffness of the Spider Spot Weld Model

Master's Thesis in the Master's programme Applied Mechanics

JOEL ANDERSSON
JONATAN DELESKOG

Department of Applied Mechanics
Division of Material and Computational Mechanics
CHALMERS UNIVERSITY OF TECHNOLOGY
Göteborg, Sweden 2014
Master's thesis 2014:22

MASTER’S THESIS 2014:22

Fatigue Life and Stiffness of the Spider Spot Weld Model

JOEL ANDERSSON

JONATAN DELESKOG

Department of Applied Mechanics
Division of Material and Computational Mechanics
CHALMERS UNIVERSITY OF TECHNOLOGY

Göteborg, Sweden 2014

Fatigue Life and Stiffness of the Spider Spot Weld Model

JOEL ANDERSSON

JONATAN DELESKOG

Master's Thesis 2014:22
ISSN 1652-8557
Department of Applied Mechanics
Division of Material and Computational Mechanics
Chalmers University of Technology
SE-412 96 Göteborg
Sweden
Telephone: + 46 (0)31-772 1000

Cover:
A spot weld joining two metal sheets in a FE model with Spider representation. See Section 3.2.3

Printed by Chalmers reproservice.
Göteborg, Sweden 2014

Fatigue Life and Stiffness of the Spider Spot Weld Model
Master's Thesis in the *Master's programme Applied Mechanics*

JOEL ANDERSSON
JONATAN DELESKOG
Department of Applied Mechanics
Division of Material and Computational Mechanics
Chalmers University of Technology

ABSTRACT

Spot welding is the main joining technique in car bodies. A typical car body contains approximately 4000 spot welds. This motivates a good knowledge of the behaviour of spot welds and a spot weld model that is easy to implement in FE car body models.

An accurate FE model for spot welds is essential in the virtual CAE design of a car body. Several ways to model spot welds exist, using both analytical solutions and explicit numerical methods. A model for fatigue evaluation should capture the failure modes of the spot welds occurring in a car body and assess fatigue life accurately.

In this study the Spider spot weld model is studied. The model is correlated with respect to stiffness tests of both coupon specimens and a complete car body. Static and dynamic stiffness for Lap Shear and Coach Peel specimens were measured and stiffness data for a car body was available at Volvo Cars. The fatigue life of the spot welds is assessed using two different methods. One is based on analytical assumptions for the stress range and one uses the stress range calculated in a FE model at the weld line.

The stiffness of the Spider model is verified at both coupon and car body level. The fatigue life assessment is however yet to be verified. Predicted fatigue life is within a factor 2-3 of tested fatigue life using both assessment methods but a large number of spot welds were also predicted to fail that did not fail in fatigue tests.

Keywords: Spot Weld, Spider Model, Fatigue Analysis, Stiffness Experiments, Correlation, Car Body, Finite Element Analysis

Contents

Preface

The work for this master's thesis was carried out during the spring of 2014 at CAE Durability Body and Trim Volvo Car Corporation. The thesis is the final part of the examination in the master's program Applied Mechanics at Chalmers University of Technology.

First of all, we would like to thank our supervisor Åsa Sällström, PhD at Volvo Cars for her consistent support, guidance and devotion throughout the work. A special thank you is sent to Mikael Fransson at the Materials centre at Volvo Cars for his assistance and instructions during our stiffness tests.

Additionally we would like to thank Lennart Josefson, professor at the department of Applied Mechanics and examiner of our thesis for his guidance during the work. We would also like to thank the staff at CAE Durability for all the help we received and for a friendly working environment.

Göteborg, June 2014

Joel Andersson & Jonatan Deleskog

1 Introduction

1.1 Background

The main advantages of the spot welding technique are time efficiency, no need for additional filler material and that the process is highly suitable for automation. For these reasons, spot welding is widely used in the automotive industry. A typical car body has approximately 4000 individual spot welds. In the contemporary competitive car industry, weight reduction is essential and thinner sheet metal is used today compared to 30 years ago. The thinner metal sheets now used have led to higher stresses, especially at spot welds [1].

Virtual product development and the use of numerical methods are important when developing new cars in order to decrease the time to market. The ability to predict fatigue life and identify critical spot welds before building the first physical prototype reduces costs significantly. This motivates a good knowledge of the behaviour of the spot welds and a model that is easy to implement into FE models.

During the past 20 years, several different spot weld modelling techniques have been developed and used in the automotive industry. They are used differently in different FE-applications, simulating durability, crash and NVH (Noise, Vibration, Harshness). The development has been controlled and driven by the continuously growing computational power and software development. At the department CAE Durability body and trim at Volvo Cars the current way to model spot welds is the *Area Contact Model 2* (ACM2) modelling technique. A drawback of this method is that the results from the analysis are mesh dependent. The performance of the weld is strongly dependent of its location relative to the mesh and how it connects to surrounding elements. This results in the need to manually examine the welds and verify their connections. Further, to get correct static and dynamic stiffness, different parameter settings need to be used. This is time consuming and a possible source of error.

The Spider spot weld model is an alternative to the ACM2 model, which has the advantage of mesh independency. In order to investigate the possibility to use this model at Volvo Cars some studies have been performed. A study with respect to fatigue was performed in 2007 and the results were promising [2]. However, later studies have shown that the predicted fatigue life with the Spider model differs from the results using the ACM2 model to a larger extent than expected. A deeper study of the Spider model is needed in order to investigate if the Spider model can be used at a larger scale at Volvo Cars Durability department and act as a substitute for the ACM2 model.

1.2 Objective

This thesis aims at reviewing the parameters of the Spider model to facilitate a correct calculation of static and dynamic stiffness and correct fatigue life prediction for a car body. This procedure will also give a better understanding of the model and its limitations. It is desired that the updated model gives correct stiffness and fatigue life in simulations.

1.3 Boundaries

Torsion of the spot welds will not be considered since when the spot welds are placed in the car body, they are placed close to another spot weld in an as high extent as possible in order to prevent torsional loading of the spot welds. Another reason is that reference torsional stiffness and fatigue data is cumbersome to extract.

The FE analyses will be limited to use MSC Nastran, which implies that the outputs of interest will be calculated according to Nastran routines.

1.4 Problem

The Spider model predicts non-expected fatigue life at Volvo Cars [3]. A cause of these deviations has not been found, but one hypothesis is that the stiffness of the Spider model is incorrect. The stiffness is here mainly referred to the stiffness of a car body modelled with Spider spot welds. A thorough analysis of the Spider model is needed. A recalibration can reveal possible errors and give further understanding of the model.

2 Method

The thesis comprises stiffness studies of the Spider model at coupon level and at complete car body level and a fatigue study at complete car body level. The work flow of the thesis can be seen in *Figure 1* and is described below.

The study starts with physical tests on two different types of coupons. The test data is used to correlate the static and dynamic stiffness of the Spider model in corresponding FE models of the coupons. The stiffness analysis continues at car body level, where test data from stiffness tests of a Volvo V70 car body is available at Volvo Cars. Similarly to the study at coupon level, the test data is used for correlation when simulating a corresponding FE model of the V70 car body containing Spider spot welds. The static and dynamic stiffness of the Spider model is evaluated and tuned for coupon and complete vehicle results. When tuning the Spider model, available parameters for modification is the modulus of elasticity, cross sectional diameter, area moment of inertia and torsional constant of the spot weld.

When studying and analysing the fatigue life of the Spider model the same V70 car body as in the stiffness study is used, since also fatigue test data is available at Volvo Cars for this car body.

The fatigue test data consists of fatigue life of 32 individual spot welds from both constant and variable amplitude tests. Two different methods of stress extraction are used to create Stress-Life graphs of the test data and to investigate the distribution of the scatter. The least square method is used to create fitted S-N curves to the test data. S-N curves established from fatigue coupon tests are available at Volvo Cars and are used as reference.

The two different stress extraction methods are used together with corresponding S-N curves developed in this study and S-N curves used today at Volvo Cars to predict fatigue life of all spot welds in the V70 car body. Prediction intervals, standard deviation, histograms and false positives are studied in the analysis as quantitative fatigue measures. False positives are here referred to as spot welds that are predicted to fail in simulations, but do not fail in physical tests.

Throughout the stiffness and fatigue analyses the results are not only compared to physical tests, but also to corresponding results from the currently used ACM2 model. In this way it is possible to evaluate the results against another spot weld modelling technique and evaluate the relevance of replacing the currently used model.

The coupons and the car body are modelled in the pre-processor Beta CAE Systems: ANSA v14.2.1 [4]. The coupons are modelled from scratch and a car body containing ACM2 spot welds is remodelled with the Spider model. MSC Nastran v2012.2 [5] is used for the FE simulations and nCode DesignLife v8.0 [6] for fatigue life predictions. The post-processor Meta v.15.0.0 is used to visualise results and Matlab is used to read results, calculate stresses and to create S-N plots, histograms and stiffness graphs.

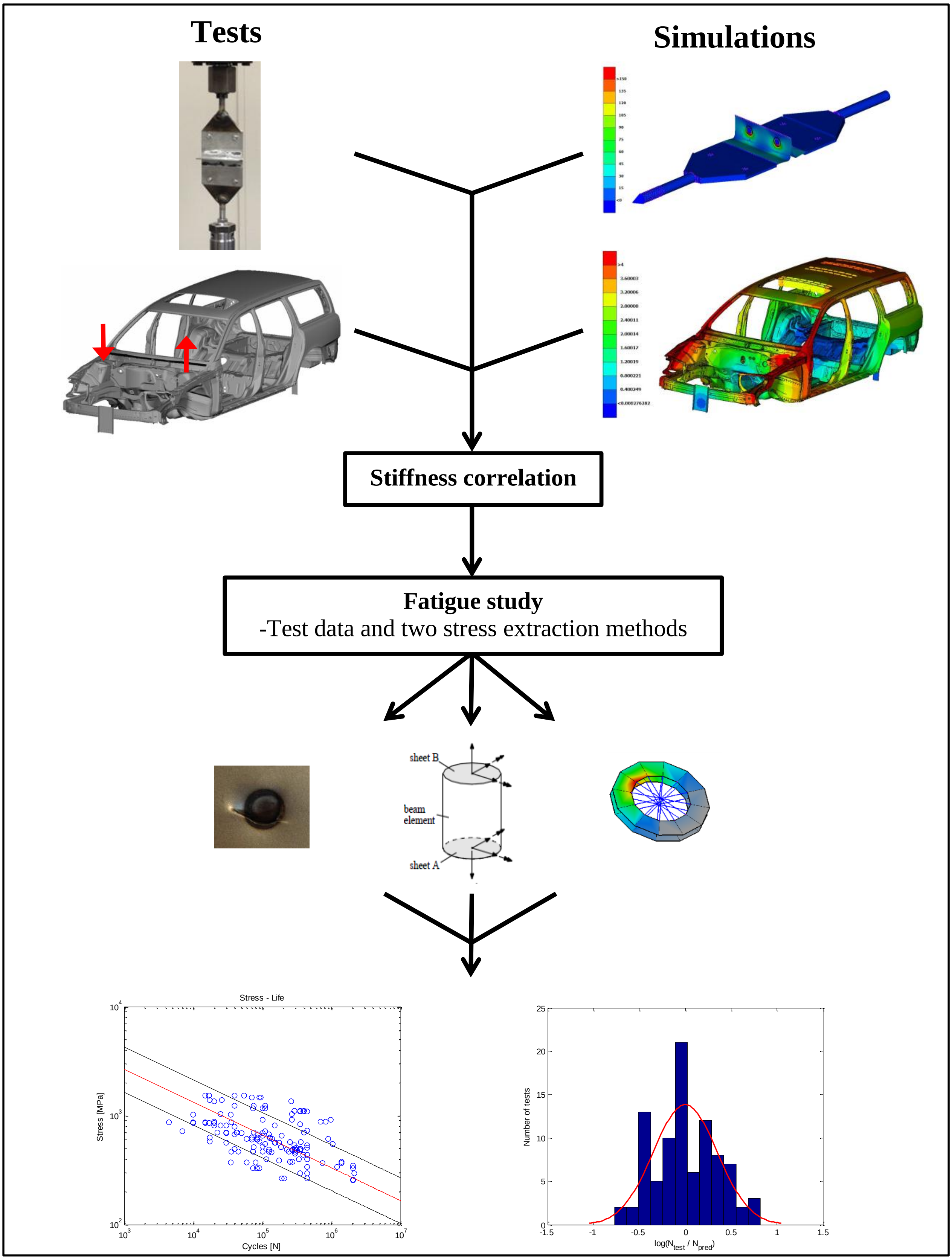

Figure 1. Work flow representative for the study.

3 Spot weld theory

3.1 Failure mechanisms

Fatigue failure of spot welds occur in different failure modes. These depend on the type of loading, the load ratio and the size of the nugget. Spot welds in a car body do not typically fail in the nugget due to fatigue, instead the surrounding sheet metal fails [1]. Figure 2 shows two different failure modes of a spot weld representative for a car body. Crack propagation paths are indicated by *I*, *II* and *III*.

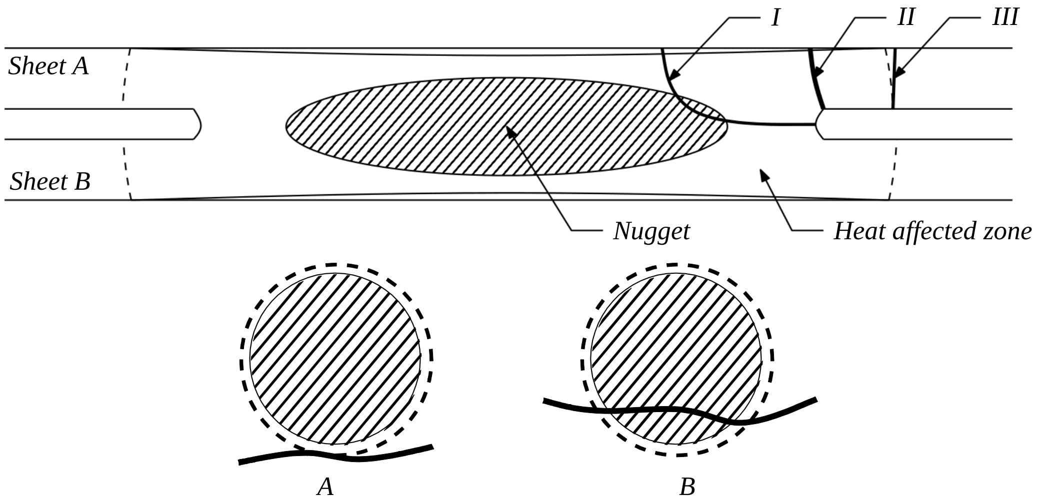

Figure 2. Side and top view of different failure modes. (A) Eyebrow crack in sheet metal at notch or in base material (II and III) (B) Typical peel crack in notch and nugget (I).

A spot weld subjected to shear dominated load typically fail according to case A. If the load is dominated by bending or peel the weld typically fail according to case B. Considering the fatigue failure of the spot welds it is crucial to have an FE model that captures the stress in the vicinity of the weld which is causing the crack initiation.

3.2 FE modelling

The first widely used spot weld modelling technique was the P2P (Point 2 Point) method. Later the ACM2 model was developed, which also is the currently used method at Volvo Cars CAE Durability Body and Trim. A third spot weld model is the Spider model. These three spot weld models can be seen in Figure 3 and are described in subsequent sections.

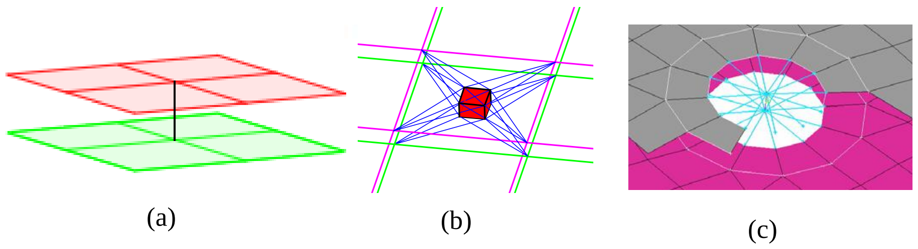

Figure 3. (a) P2P. (b) ACM2. (c) Spider.

3.2.1 P2P – Point to Point

This method connects the shell elements by a single beam element, which represent the spot weld nugget. A major drawback of this method is that the two sheets need to have coincident meshes, i.e. this method is highly mesh dependent. Also, the beam element connects only to one node in each sheet. An effect of this is that stress concentrations are introduced. For fatigue analyses forces and moments in the beam element are extracted. Radial stresses in the adjoining sheets are calculated according to an analytical expression, as described in Section 3.2.3. The calculated radial stresses are used to assess the fatigue life of the spot welded joints.

3.2.2 ACM2 – Area Contact Model 2

The ACM2 model was developed to circumvent the mesh dependency described in the P2P method. The model consists of an eight node solid element which represents the nugget, (CHEXA in Nastran), connected to the surrounding mesh by kinematic coupling constraints (RBE3 in Nastran), blue elements in Figure 3 (b). These interpolation constraints are expressed using the shape functions of the shell elements and the displacement of the connected nodes [7]. Different area scale factors are used in different kinds of analyses when using the ACM2 model, determining the size of the CHEXA element.

The command MPCFORCE in Nastran outputs the forces and moments in a global coordinate system at the corner nodes of the CHEXA element. Figure 4 describes how the quantities are transformed to a local coordinate system and further to a centroid representation on the CHEXA element. This calculation procedure can for example be obtained in nCode DesignLife [6]. Once the centroid forces and moments are obtained, the same procedure as in the P2P method can be used to calculate the radial stress in the sheet metal surrounding the spot weld. The ACM2 model is easy to create with no need to adjust the mesh. However, the calculated results will vary if the geometry is remeshed, if the RBE3 elements are connected to a radius or if spot welds located close to each other share connection nodes of the RBE3 elements.

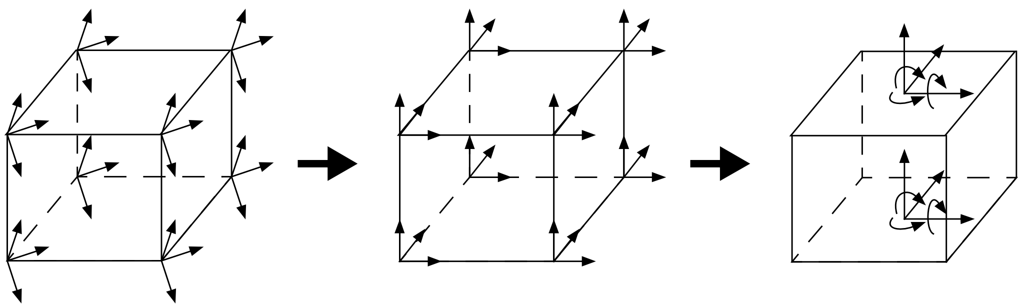

(a) (b) (c)

Figure 4. (a) Quantities in a global coordinate system. (b) Quantities in a local coordinate system. (c) Centroid representation of quantities [6].

3.2.3 Spider model

This method was proposed to eliminate the dependency of the element mesh seen in the ACM2 model. A rigid area equal to the size of the spot weld is created by rigid elements (RBE2 in Nastran) in a spoke pattern in each steel sheet. The rigid elements are oriented from the centre of the nugget to the weld line. The rigid areas are connected by a beam element (CBAR in Nastran), similar to the P2P method, see Figure 5. Available parameters for modification of the CBAR element are the modulus of elasticity, cross sectional diameter, area moment of inertia and torsional constant.

By creating a circle of elements around the weld line of equal size the most adjacent elements for all spot welds will be identical. These elements (CQUAD4 in Nastran) are denoted Zone 1 in Figure 6. This is desirable since the result from analyses will be more accurate with good quality elements. The number of wedges in the model determines in how many points the stress can be evaluated along the weld line.

The default settings of the Spider model follow from earlier studies and standards performed and evaluated at Volvo Cars. The number of rigid elements in the nugget is set to 12 and the length of Zone 1 in radial direction is 2 mm for all sizes of spot welds [8]. The overall mesh size needed to accommodate this without allowing too large differences in element length is 2.5 mm.

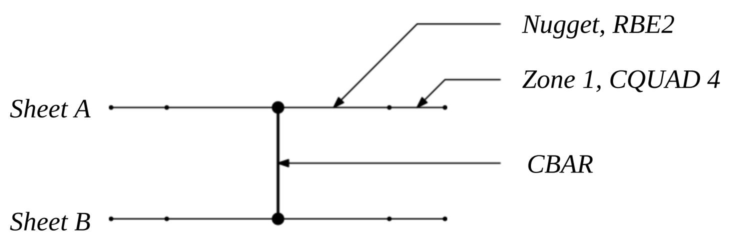

Figure 5. Side view of the Spider model with nugget and Zone 1.

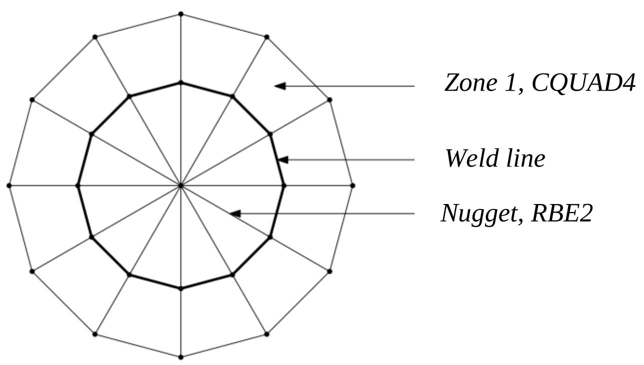

Figure 6. Top view of the Spider model with twelve rigid wedges and Zone 1.

Structural stress acting in the vicinity of the weld can be extracted using different methods. Two methods are studied here. Both methods aim at estimating the stress acting at the weld line. This stress is considered to cause the fatigue failure of the nugget and the surrounding sheet material seen in Figure 2 [9].

Cubic stress assessment
By utilizing the displacement and rotations in the elements of Zone 1 it is possible to extract the nodal stresses at the weld line. The maximum nodal principal stress acting at the weld has proven to be a good measure of the structural stress [2, 10]. By using the nodal displacement it is possible to evaluate the principal stresses with the strain gauge approach [6]. In Figure 7 a quarter of a Spider model is shown with a definition of a local coordinate system,$(xy)'$, and a global coordinate system, (xy).

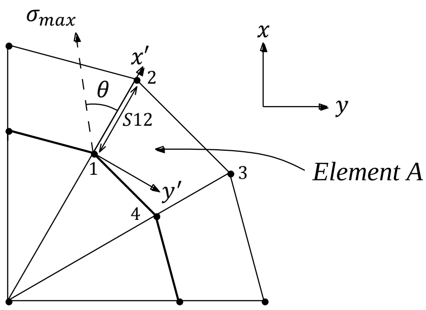

Figure 7. A quarter of the Spider model with defined local coordinate system.

The nodal displacement and rotations of the Zone 1 elements expressed in the global coordinate system are transformed to the local coordinate system. Looking in element A, in Figure 7, the goal is to calculate the strain in node 1 in the directions of node 2, 3 and 4 using the displacements and rotations of the element. These three strains are used to determine the strain tensor acting in node 1. The calculation of the strains in direction of the three node pairs is considered to be a one dimensional problem. It is assumed that the segment of the elements in these directions deforms with a cubic shape. The local strain tensor is established for the nodes. The corresponding global strain tensor is calculated and the resulting stress components acting can be obtained via Equation 1-5. The stress is evaluated in both the top and bottom of the shell.

$$\sigma_{xx} = \frac{E}{1-\nu^2}\left(\epsilon_{xx} + \nu\epsilon_{yy}\right) \tag{1}$$

$$\sigma_{yy} = \frac{E}{1-\nu^2}\left(\epsilon_{yy} + \nu\epsilon_{xx}\right) \tag{2}$$

$$\tau_{xy} = \frac{E}{1+\nu}\epsilon_{xy} \tag{3}$$

The material properties E and ν are chosen according to the sheet material. The principal nodal stress and the orientation relative to the x-axis are calculated as:

$$\sigma_{1,2} = \frac{\sigma_{xx}+\sigma_{yy}}{2} \pm \sqrt{\left(\frac{\sigma_{xx}-\sigma_{yy}}{2}\right)^2 + \tau_{xy}^2} \tag{4}$$

$$\theta = \frac{1}{2}\tan^{-1}\left(\frac{2\tau_{xy}}{\sigma_{xx}-\sigma_{yy}}\right) \tag{5}$$

This stress is used when evaluating the stress range in the Absolute Maximum Principle method [6]. The highest stressed node along the weld line of sheet A and B is considered to be the location of crack initiation. The output command STRESS(CUBIC) in MSC Nastran extracts these stresses. It is important to note that the assumptions regarding the cubic deflection of the segments of the CQUAD4 elements require that the deformation is small.

Analytical stress assessment

Another relevant stress extraction method is to calculate the radial stress in the adjacent sheet metal using the forces and moments transferred through the weld by the beam element, i.e. equivalent to the calculations in the P2P and ACM2 modelling technique. This method is based on an analytical solution [11]. A free body diagram of the beam element connecting the sheets is seen in Figure 8 (a). Figure 8 (b) shows an assumption of a rigid kernel in the centre of a large plate. This assumption leads to Equation (6) - (10) representing the stress in the sheet metal along the circumference of the nugget. The maximum stress range is found at the angle θ.

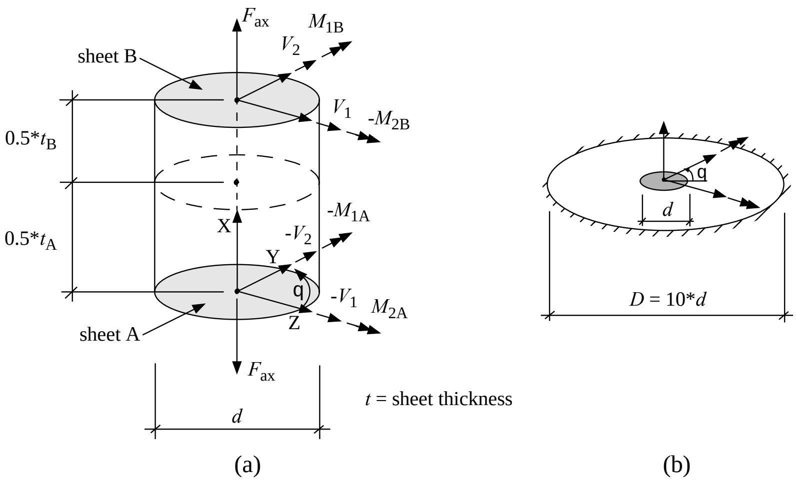

Figure 8. (a) Free body diagram of the beam element. (b) Assumption of a rigid kernel in the centre of a large plate [7].

Stress resulting from shear force V_i:

$$\sigma_{max}(V_i) = \frac{V_i}{\pi d t_j} \qquad i = 1{,}2 \qquad j = A, B \tag{6}$$

Stress resulting from axial force F_{ax}:

$$\sigma(F_{ax}) = 0.6\sqrt{t_j}\ \frac{1.744F_{ax}}{{t_j}^2} \qquad if\ F_{ax} > 0 \qquad j = A, B \tag{7}$$

Stress resulting from bending moment M_{ij}:

$$\sigma_{max}\left(M_{ij}\right) = 0.6\sqrt{t_j}\ \frac{1.872M_{ij}}{d{t_j}^2} \qquad i = 1{,}2 \qquad j = A, B \tag{8}$$

The stress distribution around the spot weld is assumed to vary as a function of sine and cosine:

$$\sigma_r{}^A = -\sigma_{max}(V_1)cos\theta - \sigma_{max}(V_2)sin\theta + \sigma(F_{ax}) - \sigma_{max}(M_{2A})sin\theta - \sigma_{max}(M_{1A})cos\theta \tag{9}$$

$$\sigma_r{}^B = \sigma_{max}(V_1)cos\theta + \sigma_{max}(V_2)sin\theta + \sigma(F_{ax}) - \sigma_{max}(M_{2B})sin\theta - \sigma_{max}(M_{1B})cos\theta \tag{10}$$

Stress Correction factors

In previous work it has been concluded that the life of a spot weld is different depending on if the load is peel or shear dominated [1]. This effect is taken into account by introducing a stress correction factor with respect to the degree of bending. In general the life of a spot weld exposed to bending stress is longer than for welds exposed to membrane stress.

Several studies have been performed regarding how these effects can be implemented in order to evaluate the fatigue life. The correction for the stresses in the Cubic stress assessment approach utilizes two S-N curves, which have been fitted to bending and membrane fatigue data respectively [12]. By defining a bending ratio of the loading condition it is possible to interpolate between a stiff and flexible design curve and assess the fatigue life of the spot weld [6].

For the analytical stress assessment a bending stress correction is often employed by the factor $0.6\sqrt{t_j}$ in Equation 7-8. This factor is based on empirical studies of fatigue specimens [11].

Another phenomenon that has been observed is that the thickness of the sheets also influences the fatigue life [1]. There are several methods to account for this. In general sheets with a larger thickness results in increased crack propagation and a lower life. The method used in this study is based on an approach where crack propagation in specimens is studied [10]. It uses a theoretical expression dependent on the structural stress range and the sheet thickness, see Equation 11.

$$S_G = \Delta\sigma \cdot s\,, \qquad s = t^{\left(\frac{m-2}{2m}\right)} \tag{11}$$

Here t is the sheet thickness and m is a material parameter, usually $m \approx 3$ for steel [13]. An additional alternative is to only use the thickness correction when the thickness exceeds a reference thickness according to Equation 12.

$$s = \begin{cases} 1 & t < t_{ref} \\ \left(\frac{t}{t_{ref}}\right)^{\frac{m-2}{2m}} & t > t_{ref} \end{cases} \tag{12}$$

In this study t_{ref} is chosen to 1 mm according to the default settings in DesignLife [6].

4 Stiffness

Static and dynamic stiffnesses are calculated and iterated using different settings of the modulus of elasticity, cross sectional diameter, area moment of inertia and torsional constant of the CBAR element. One approach is to change these settings independently of each other and another is to specify a diameter and let the area moment of inertia and torsional constant follow from analytical expressions corresponding to chosen diameter. In this way all parameters influencing the stiffness of the Spider spot weld model are examined. To examine the stiffness of the individual spot weld, simple structures, or so called coupons are used.

4.1 Coupons

Two types of specimens are used in this study, Lap Shear and Coach Peel coupons, with two spot welds on each specimen. The geometry of the test specimens can be seen in Figure 9. In total three Lap Shear specimens and three Coach Peel specimens are tested. They are referred to as *LS1*, *LS2*, *LS3* and *CP1*, *CP2*, *CP3*. The spot weld diameter is 5.6 mm for both specimens and the sheet material is steel representative for a car body with sheet thickness of 1 mm.

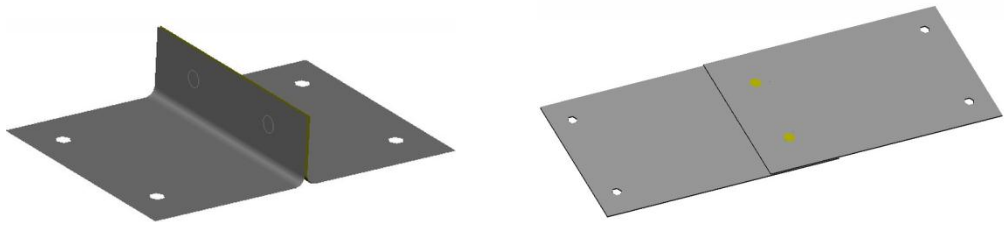

(a) (b)

Figure 9. (a) Coach Peel specimen. (b) Lap Shear specimen.

4.1.1 Test Setup

The coupons are welded and bolted onto custom made grips. The grips have threaded rods and are mounted in a servo-hydraulic test system. A mounted specimen is shown in Figure 10 with denoted parts of the test equipment.

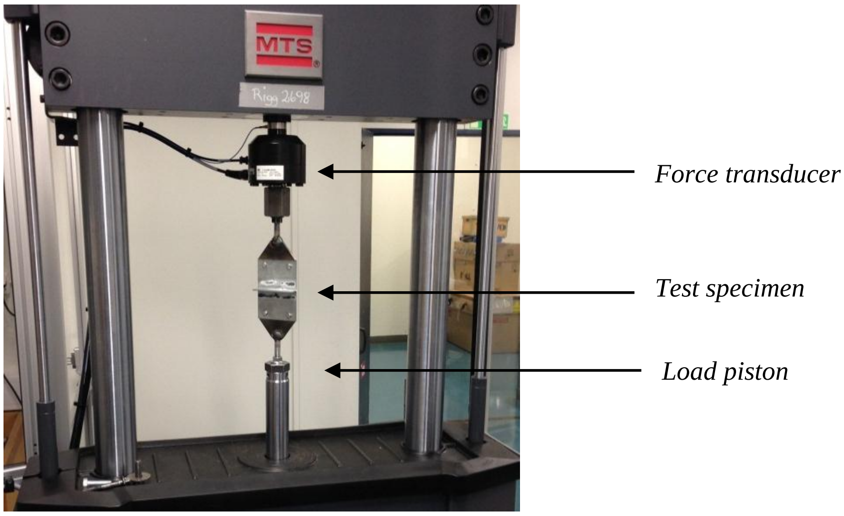

Figure 10. Coach Peel test setup.

Static and dynamic tests are performed in order to investigate any possible dynamic effects of the stiffness. Specific test conditions are listed in Appendix A. The testing aims at finding the stiffness in the elastic region and therefore loads that do not introduce plastic deformation are used. The dependence of amplitude in the dynamic tests are investigated using the load ratios $R_1 \approx 0.1$ and $R_2 \approx 0.4$. The reason not to introduce any compressive load is to avoid the risk of buckling.

Displacements and forces are recorded in both the static and dynamic test. In the dynamic test, stiffness is measured at every frequency level with an increment of 1 Hz. The chosen frequency range of 1-100 Hz is based on that a car body does not experience loads excited at frequencies higher than 60 Hz during normal operation. The applied force in the test rig is recorded by a force transducer and the displacement is measured by the position of the load piston. Stiffness is calculated according to Equation 13.

$$K = \frac{F}{\delta} \tag{13}$$

The static stiffness is measured using two load rates in order to reveal any damping or relaxing behaviour in the coupons. The force is ramped linearly over the force range.

4.1.2 FE models

The coupons are modelled together with the grips in order to capture any static or dynamic influence of the test setup. The sheet metal is modelled with shell elements with a mesh resolution of 2.5 mm whereas the grips are modelled with solid elements. The coupons are loaded along the grips in one end, see Figure 11 and 12. This end is constrained in all directions except the loading direction. The other end is clamped. In the Coach Peel model, rigid RBE2 elements are connecting the top edge of the flange to simulate contact during deformation. Simulations with and without these RBE2 elements are performed. The weld and bolt connections are also modelled by rigid RBE2 elements.

The static solution is calculated using Nastran SOL101, where a static load equal to the maximum applied force in the test was used. Since the displacement in the test only occurs in the elastic region, the stiffness is constant and not sensitive to chosen load level.

The dynamic analysis superimposes a static solution using SOL101, representing a constant pre load, and a modal frequency analysis using SOL111, which represents the amplitude load with increasing frequency. The superposition is possible since the analysis is linear.

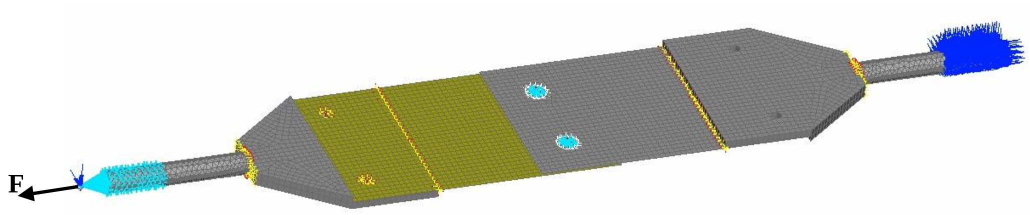

Figure 11. FE model of the Lap Shear specimen.

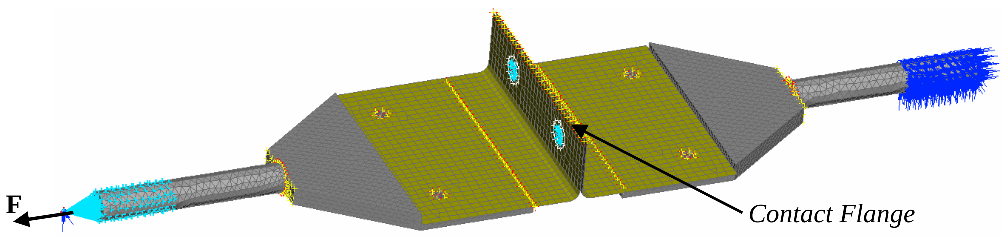

Figure 12. FE model of the Coach Peel specimen.

4.1.3 Results

The results from the static tests are shown in Table 1 and 2. The stiffness for LS2 is significantly higher compared to the other specimens. This test was not considered to be reliable due to incorrect settings in the test equipment software. The CP2 specimen was tested under correct circumstances but differs compared to the other coupons. But since CP1 and CP3 show identical results it is assumed that their stiffness is most representative. The coupons are prepared manually and geometrical difference within the specimens of the same type occurs. This is considered as a reason to scatter in the test data.

Table 1. Lap Shear static stiffness test results.

Test Specimen	**Run**	**Load Rate** [mm/min]	$\mathbf{K_{static}}$ [N/mm]
LS1	1	0.01	27700
	2	0.02	30100
	3	0.02	29700
	4	0.01	29600
LS2	1	0.01	36900 *
	2	0.02	43200 *
LS3	1	0.01	30700
	2	0.02	37800

* Data not considered reliable

Table 2. Coach Peel static stiffness test result.

Test Specimen	**Run**	**Load Rate** [mm/min]	$\mathbf{K_{static}}$ [N/mm]
CP1	1	0.01	1400
	2	0.02	1410
CP2	1	0.01	1600
	2	0.02	1900
CP3	1	0.01	1400
	2	0.02	1410

The static and dynamic stiffness in the FE model were examined using different properties of the CBAR element. It was difficult to correlate the stiffness for the Lap Shear specimen, but possible for the Coach Peel specimen. Using a CBAR element with diameter equal to the spot weld diameter, area moment of inertia and torsional constant associated to the diameter and a modulus of elasticity corresponding to the used sheet metal gave good results. These results can be seen in Table 3.

Table 3. Static stiffness from FE models

Specimen	$\mathbf{K_{static}}$ [N/mm]
Lap Shear	47800
Coach Peel without contact	1360
Coach Peel with contact	1420

When comparing the FE results to the tests, one can see that the static stiffness for the Lap Shear specimen is about 40 percent higher than the tested stiffness. However, the stiffness of the Lap Shear specimen is large, in the order 1/4 of the stiffness of the test rig [14]. Because of this it is difficult to measure the stiffness of the specimen with accuracy. Comparing the result for the Coach Peel specimen, one can see that the FE results are within one percent of CP1 and CP3 when using a model with contacts. When contact is not considered the stiffness is underestimated about four percent compared to the test data.

The dynamic stiffness results, which can be seen in Figure 13, show the same behaviour as the results of the static stiffness. The Lap Shear specimen FE results are far from the test results while the Coach Peel specimen results can be considered as well correlated against the test results from CP1 and CP3. At higher frequencies the dynamic effects are more prominent in the FE models, one should though keep the scale of the stiffness axis in mind when quantifying the difference. In Figure 14 the effects of simulating contact in the Coach Peel specimen can be seen, which shows similar trend as the static stiffness.

No eigen frequencies were found in the range of 1-100 Hz, but when proceeding one test of the Lap Shear specimen towards 200 Hz, an eigen frequency were found around 170 Hz. As expected, the specimen broke distinctly.

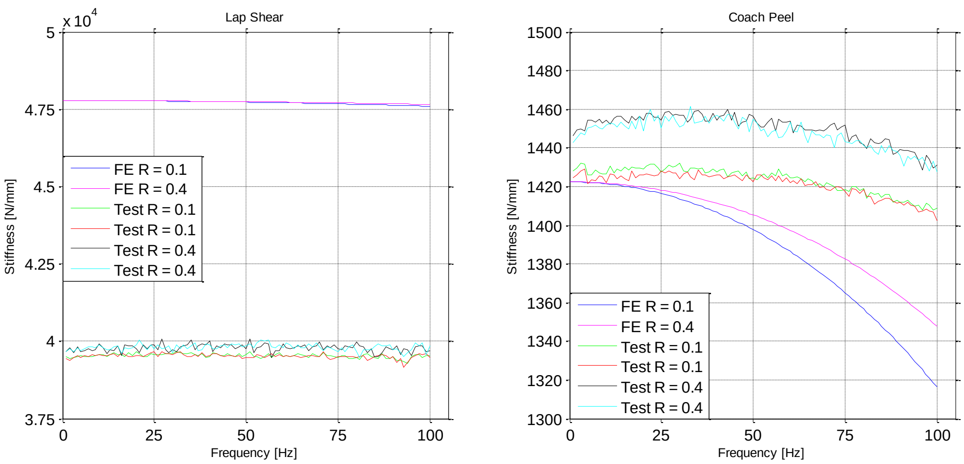

(a) (b)

Figure 13. *(*a) LS3 test data together with FE result. (b) CP1 test data together with FE results. Note the scale of the stiffness axis.

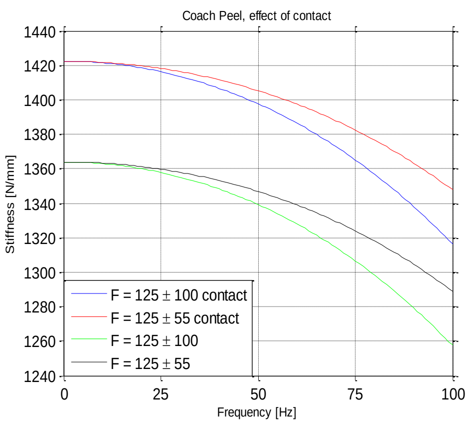

Figure 14. Coach Peel specimen with and without contact. Note the scale of the stiffness axis.

4.2 V70 Car Body

In 2002 a large correlation project including fatigue and stiffness of a V70 car body was performed within the Ford group with Volvo Cars and Jaguar Land Rover [15]. 16 Volvo V70 car bodies were tested for fatigue life and global static and dynamic stiffness. The stiffness was measured as:

- Load point and torsional static stiffness
- Eigen frequencies in test rig
- Eigen frequencies as free-free body

4.2.1 Test setup

In the tests the car body had a front pivot point attached to the front bumper. The rear of the body was attached to the floor via bending plates, which are vertically stiff but longitudinally and laterally flexible. Hydraulic actuators created a load in the front shock towers. See Figure 15 for a description of the test rig setup. This test rig setup was used for the static stiffness and body in rig eigen frequencies and when the free-free vibrations were examined the car body was suspended with soft air rubber mounts [15]. When investigating the dynamic stiffness of the car body it was excited by a soft rubber hammer.

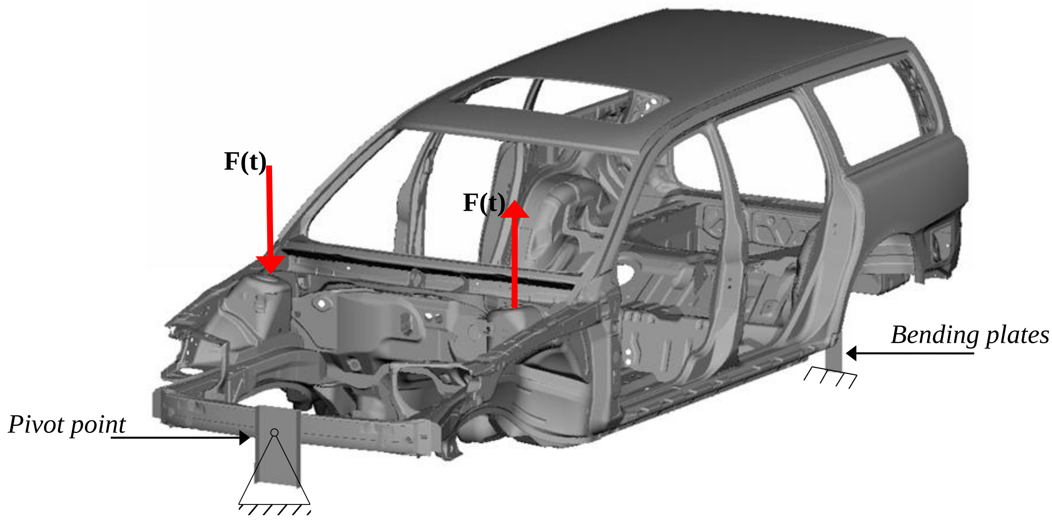

Figure 15. V70 test rig setup.

4.2.2 FE model

The FE model of the car body used in the 2002 correlation project was adopted in this study and the Spider model was introduced in it. To be able to implement the Spider model, the mesh of the car body was refined from 10 to 2.5 mm mesh density to achieve good elements connecting to the Spider model according to Chapter 3.2.3.

A thorough review of the 4150 spot welds revealed defects in the old model and locations where it was impossible to implement the Spider model. This was due to connection points located too close to edges and to each other. The remedy for this problem was to move the connection points whose inaccurate locations were obvious. The connection points which were not appropriate to move and not able to realize with the Spider model was realized with the ACM2 model instead. In total, 50 connections were left without FE-representation. These were connections mainly appearing as duplicates, here the spot weld joining the highest number of sheet metal was realized with a FE representation. The final distribution of the spot welds can be seen in Table 4. A graphical representation of the complete distribution can be seen in Appendix B.

Table 4. Distribution of spot welds in the studied model.

Type of FE representation	Number of spot welds
Spider	4063
ACM2	37
Not realized	50
Total:	4150

The static stiffness was measured as a load point static stiffness and a torsional static stiffness. The load point static stiffness was calculated at each front shock tower by measuring the static deflection when applying a load of 2000 N. The torsional static stiffness was calculated according to Equation 14.

$$K = \frac{M}{\phi} = 2 \cdot \frac{\pi}{180} \frac{(F_{LHS} - F_{RHS})L^2}{(\delta_{LHS} + \delta_{RHS})} \tag{14}$$

Here L is the horizontal distance from the pivot point to the load point and δ is the static deflection of the load point. Further small angles were assumed [15]. Nastran SOL101 was used to calculate the static stiffness. The dynamic stiffness was analysed using Nastran SOL103 for eigen frequencies and eigen modes. Meta and Matlab was used to post process the data.

To investigate how the moved connection points and the connections without FE representation influence the stiffness, the new connection coordinates were mapped onto the FE model with ACM2 spot welds used in 2002 and compared to the old connection coordinates. Table 5 clearly shows that the new connection representation did not affect the static stiffness significantly, since the change in stiffness is less than one percent. It was therefore decided that the new connection representation was applicable.

Table 5. Influence of modified connection representation.

Static Stiffness	LHS Load Point [kN/mm]	RHS Load Point [kN/mm]	Torsional [kNm/deg]
Old connection representation	0.923	0.945	11.55
New connection representation	0.918	0.939	11.49

Since the mesh resolution is changed when using the Spider model in the car body, compared to the corresponding ACM2 model, an investigation regarding how mesh size influence the stiffness was performed. The mesh was refined from 10 to 2.5 mm in a FE model with ACM2 spot welds, keeping the area scale factor and the connection nodes of the RBE3 elements. The stiffness of these two models is shown in Table 6. The stiffness is decreased with 4 percent when using a finer mesh.

Table 6. Influence of the stiffness with a refined mesh.

Static Stiffness	LHS Load Point [kN/mm]	RHS Load Point [kN/mm]	Torsional [kNm/deg]
10 mm mesh	0.923	0.945	11.55
2.5 mm mesh	0.885	0.904	11.07

4.2.3 Results

A CBAR element with diameter equal to the spot weld, area moment of inertia and torsional constant associated to the diameter and a modulus of elasticity corresponding to the sheet metal in the car body was shown to give a lower stiffness than the tests. The load point and torsional static stiffness using this CBAR element can be seen in Figure 16 and 17. The eigen frequencies for the body in rig and free-free vibrations can be seen in Figure 18 and 19. When interpreting the results, one should keep in mind that the Spider and the ACM2 model were compared having the same spot weld diameter, the same connection representation but different mesh size.

The results for the ACM2 car model are given using a specific set of parameters, which results in good correlation to the test results. It should however be mentioned that a different set of parameters are used in the ACM2 model for different types of analyses, giving worse correlation to the stiffness than the results showed.

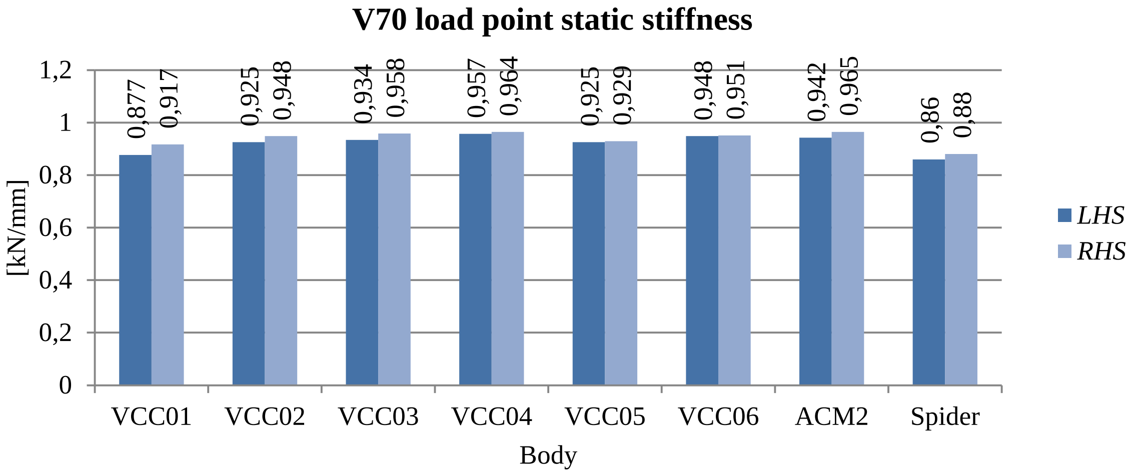

Figure 16. Load point static stiffness in six car bodies and two FE models.

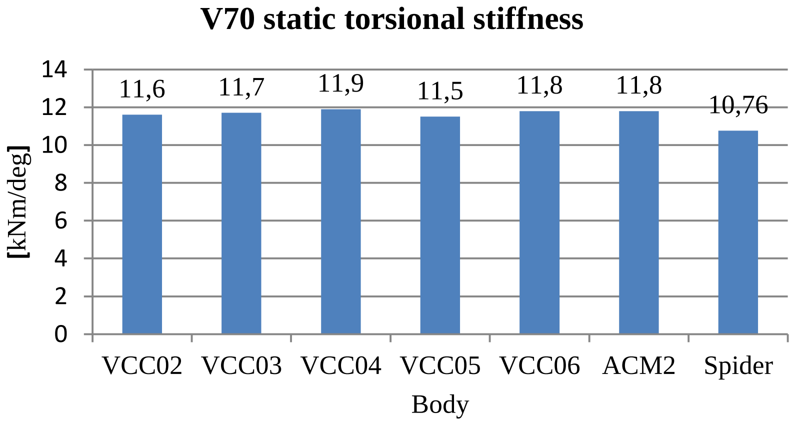

Figure 17. Static torsional stiffness in five car bodies and two FE-models.

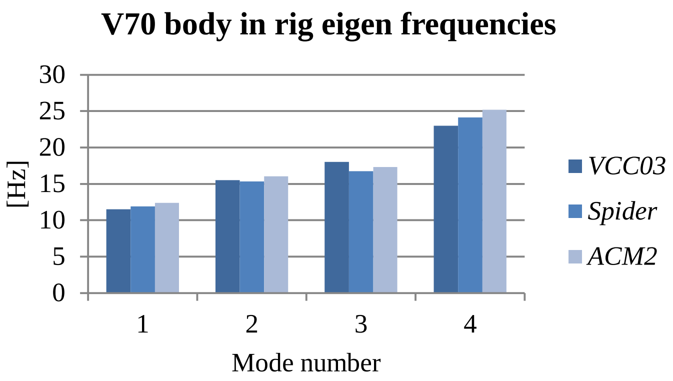

Figure 18. Body in rig eigen frequencies with corresponding mode number.

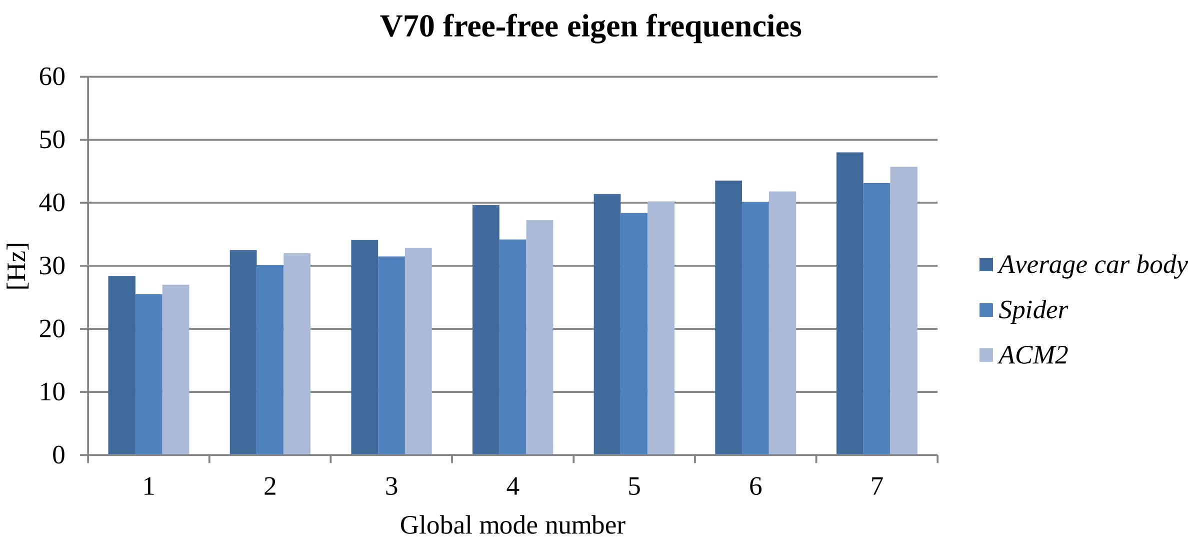

Figure 19. Free-free eigen frequencies with corresponding global mode number.

Using a CBAR element with diameter equal to the spot weld diameter or using a rigid CBAR element did not result in significantly different stiffness. When the rigid CBAR element did not give a stiff enough FE model it was examined how the stiffness quantities were influenced when increasing the area defined by the 12 rigid RBE2 elements. However, an increase of the RBE2 diameter of 1 mm did not make the car body significantly stiffer. This method was not further studied since it was difficult to create larger Spider spot weld areas because of narrow flanges in the car body.

The static stiffness of the Spider model is lower than the tested car bodies and the ACM2 model. One possible reason for this is that no contacts or friction is simulated in the FE model, i.e. the only parameter controlling the stiffness except for the sheet metal stiffness is the stiffness of the spot welds. One argument for this theory is that the Coach Peel specimen was four percent weaker when it was modelled without the rigid elements on the flange simulating contact. The stiffness of the Spider car body FE model is eight percent lower than the average stiffness of the tested car bodies, i.e. it shows the same behaviour as the Coach Peel specimen.

Another reason that the car body modelled with Spider spot welds is weaker than the corresponding ACM2 model is the refined mesh. In general a smaller element size implicates a weaker solution [16]. This was confirmed with a comparison between two models. A car body with a mesh resolution of 2.5 mm showed a decrease in stiffness of four percent compared to a model with 10 mm mesh resolution, as seen in Table 6.

Regarding the body in rig eigen frequencies the trend is that the FE models are stiffer than the tested car body. One reason for this is that the car body is mounted on a girder table while the constraints in the FE model are infinitely rigid. Mode number three is a front vertical bend mode and is dominated by bumper beam rotation. An explanation to why both FE models have a lower eigen frequency than the tested car body for this mode is that no contact is modelled between the bumper beam and the side members [15]. The mode shape of mode 2 is less affected by spot weld parameters than mode 1 and 4 and the simulated eigen frequency is close to the tested. The eigen frequencies for the free-free vibrations follows the trend that the Spider FE model is weaker than the tested car bodies and the ACM2 FE model.

4.3 Stiffness conclusion

The stiffness study on coupon as well as complete car body level shows that using a CBAR element with diameter equal to the spot weld diameter, area moment of inertia and torsional constant associated to the diameter and modulus of elasticity corresponding to the sheet metal gives reasonable stiffness for both static and dynamic load cases. The parameters of the CBAR element did not have to be changed independently in order to achieve these results. The stiffness for the Coach Peel specimen shows a good correlation to the test data.

The concluded settings of the CBAR element are actually the settings used in earlier studies of the Spider model at Volvo Cars. The hypothesis that the non-expected predicted fatigue life for the Spider model should origin from an incorrect stiffness could therefore not be verified.

5 Fatigue

The correlation project performed in 2002 serves as a foundation for the fatigue part of this study, in contrast to earlier studies of the Spider model that were based on fatigue coupon tests. Fatigue life of 32 individual spot welds is available from the correlation project and is used when evaluating predicted fatigue life.

5.1 Test Setup

The same test set up was used as described in Chapter 4, scaling the load in the front shock towers by both constant and variable amplitudes. The variable amplitude force signal is a completely reversed signal recorded at Volvo Cars endurance test track, see Appendix C for a graph of the signal. The tests were performed at quasi-static loading rate using a frequency of 3 Hz. As a rule of thumb, quasi-static loading is achieved when a frequency lower than the lowest eigen frequency divided by three is used [17].

5.2 FE simulations

The V70 FE model built with Spider spot welds was exposed to constant and variable amplitude loading corresponding to the fatigue tests. The 32 individual spot welds mentioned previously were analysed using the Cubic stress assessment and the Analytical stress assessment described in Section 3.2.3. The stresses for constant amplitude loading were extracted and plotted against the corresponding fatigue life from the tests and an S-N plot was created, see Figure 21 and 23. S-N curves were established by performing curve fits by the least squares method (LSQ) with respect to the fatigue life. These new S-N curves were used to predict fatigue life of all spot welds in the car body. The cubic and analytical stress assessment methods are utilized in the Seam Weld and Spot Weld Module in DesignLife respectively. Figure 20 describes the method for fatigue life evaluation for the cubic and analytical stress assessment in DesignLife. Both the Spot Weld and Seam Weld Module use rain flow cycle counting and Palmgren Miner summation rule for variable amplitude loading.

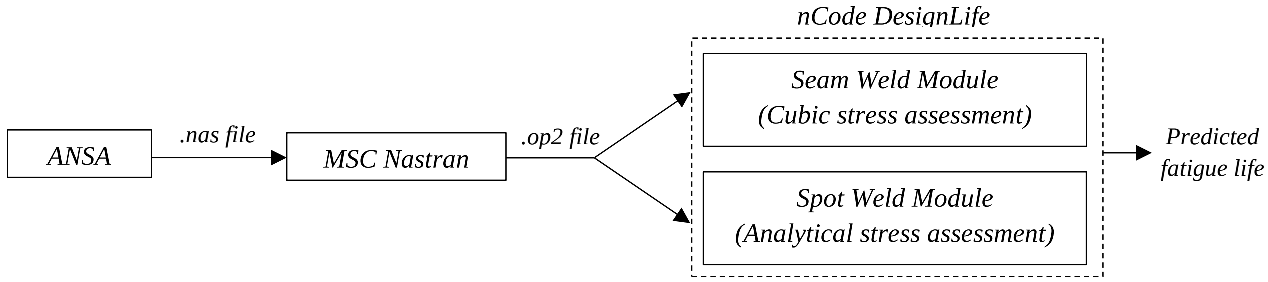

Figure 20. Flow chart of the method used to assess fatigue life of the V70 car body.

The fatigue life of the 32 individual spot welds that failed in the tests were compared to the corresponding predicted fatigue life from simulations. Prediction intervals, standard deviation and histograms were used to compare the data. The fatigue life of the remaining ~4000 spot welds was predicted with the aim of finding false positives.

5.3 Results

The results are presented separately for the Spot Weld and Seam Weld Module. The predictions are evaluated using histograms showing the logarithm of the ratio of tested life over predicted life together with fitted normal distributions. The S-N curves are designed aiming at a mean value equal to zero in the histograms for variable amplitude loading, since this is the type of loading that an actual car body is typically exposed to. This is done instead of adjusting the damage sum.

5.3.1 Spot Weld Module

The stress ranges around the spot welds that failed in the tests are plotted against the tested fatigue life in Figure 21, together with different S-N curves. As seen in Figure 21 (c) the least square fit results in a curve whose inclination is about twice as steep as the *Spot Sheet Steel (SSS)* S-N curve in Figure 21 (a). The SSS curve is currently used at Volvo Cars and is developed from fatigue coupon tests. Figure 21 (e-f) shows corresponding results for the ACM2 model. The figures also show an interval of a factor five of predicted life using the related S-N curve.

All three S-N curves were adjusted in order to achieve a mean value equal to zero for variable amplitude in the histograms. The adjusted S-N curves can also be seen in Figure 21 and the corresponding curve parameters can be seen in Table 7. Histograms for the least square fit, SSS and for the ACM2 model can be seen in Figure 22. Prediction intervals were established by using one standard deviation for each analysed population. The prediction intervals and percentage of the population within these intervals is also presented in Figure 22.

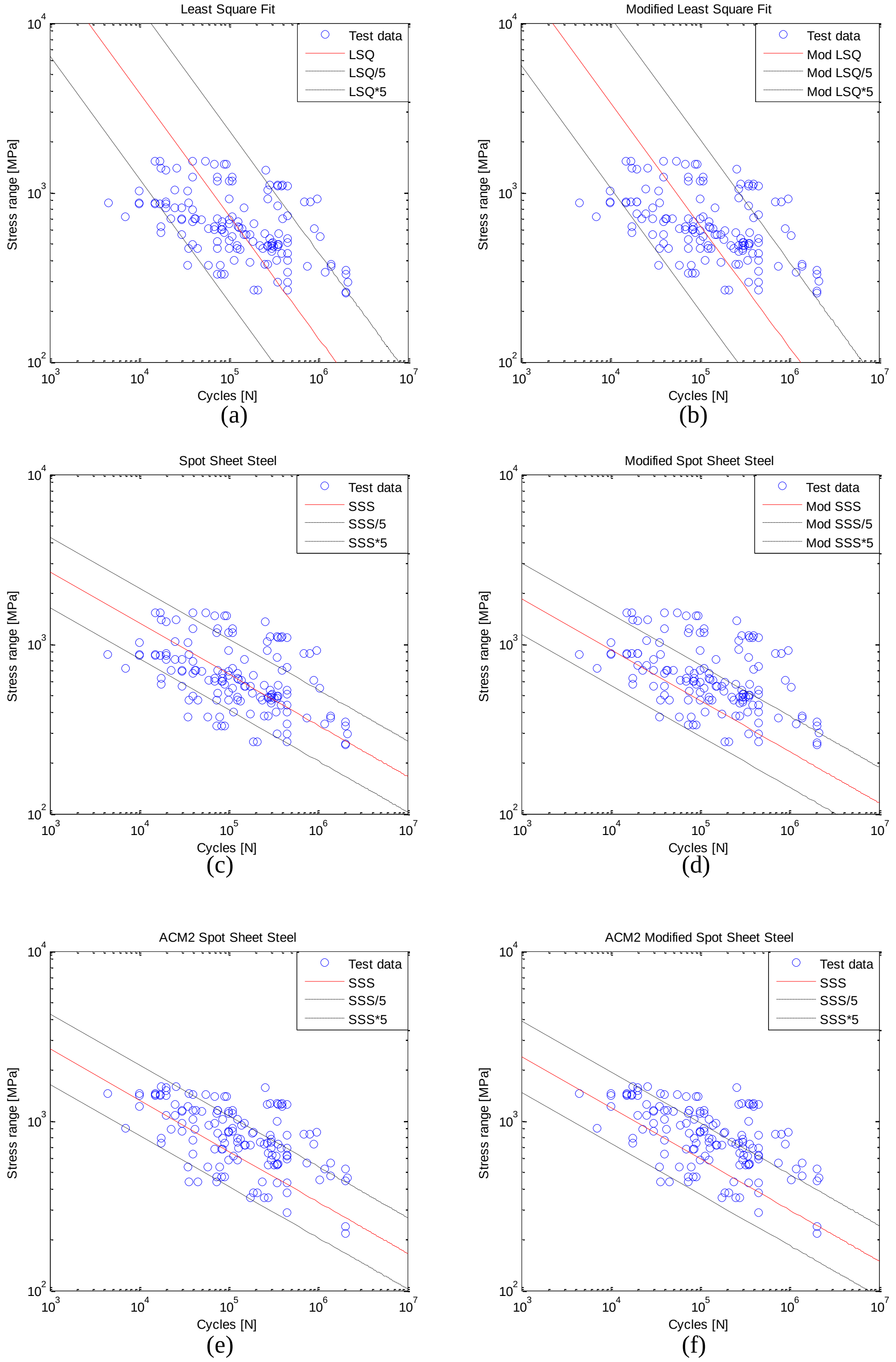

Figure 21. Test scatter, S-N curves and adjusted S-N curves for the Spot Weld Module with (a)-(b) Spider model using the least square fit, (c)-(d) Spider model using the Spot Sheet Steel curve, (e)-(f) ACM2 model using the Spot Sheet Steel curve.

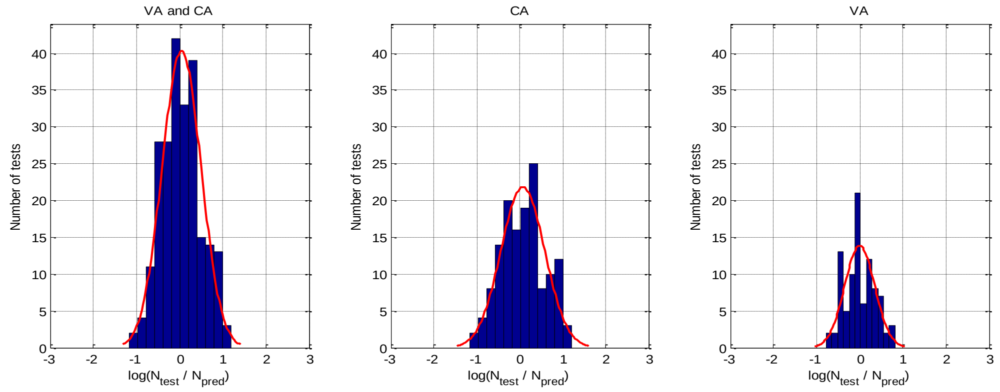

(a) m = 0.05 $0.4<N_{test}/N_{pred}<3.2$ (68%) m = 0.07 $0.4<N_{test}/N_{pred}<3.8$ (64%) m = 0 $0.4<N_{test}/N_{pred}<2.2$ (63%)

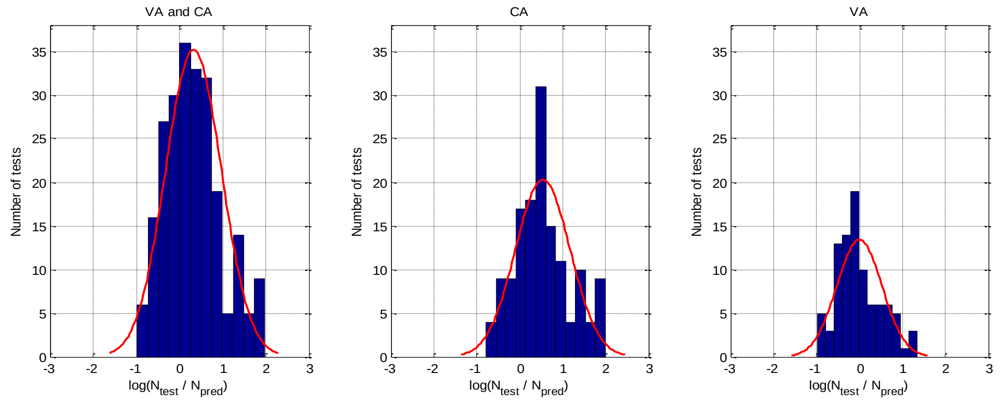

(b) m = 0.33 $0.5<N_{test}/N_{pred}<9.5$ (68%) m = 0.54 $0.8<N_{test}/N_{pred}<15$ (67%) m = 0 $0.3<N_{test}/N_{pred}<3.4$ (70%)

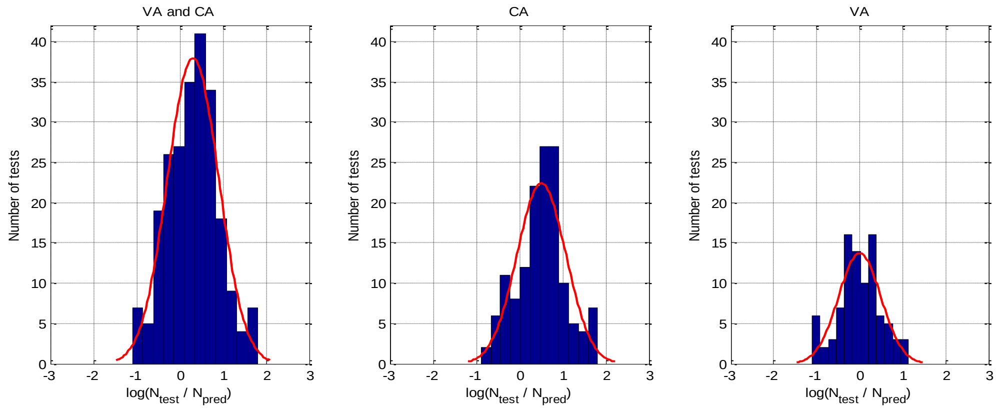

(c) m = 0.31 $0.5<N_{test}/N_{pred}<8$ (69%) m = 0.51 $0.9<N_{test}/N_{pred}<12$ (72%) m = 0 $0.3<N_{test}/N_{pred}<3.1$ (71%)

Figure 22. Histograms using the modified S-N curves for the Spot Weld Module for (a) LSQ fit, (b) SSS, (c) ACM2.

Table 7. S-N curve parameters for the Spot Weld Module, $\Delta\sigma = A \cdot N^b$.

S-N curve	A	b
LSQ curve fit	$3.02 \cdot 10^6$	-0.72
Modified LSQ curve fit	$2.67 \cdot 10^6$	-0.72
Spot Sheet Steel	$2.10 \cdot 10^4$	-0.30
Modified Spot Sheet Steel	$1.47 \cdot 10^4$	-0.30
Spot Sheet Steel ACM2	$2.10 \cdot 10^4$	-0.30
Modified Spot Sheet Steel ACM2	$1.89 \cdot 10^4$	-0.30

The false positives were investigated using variable amplitude loading. The limit defining a false positive was set to the highest lifetime a spot weld endured in the physical tests.

Some spot welds in the car body are only for manufacturing purposes, some are unrealised and some are for the test rig setup. The calculated false positives were reviewed in order to reveal only the true false positives and are presented in Table 8.

Table 8. False positives using the Spot Weld Module.

Method	False positives
Spider LSQ	≈280
Spider SSS	31
ACM2	24

The prediction interval for the least square fit is significantly better than for the Spot Sheet Steel curve and for the ACM2 model. However, the amount of false positives is increased considerably.

5.3.2 Seam Weld Module

The stress ranges acting at the spot welds are plotted against the fatigue life from the constant amplitude tests in Figure 23 (a) - (c). The S-N curves used for spot welds in DesignLife at Volvo Cars, *Spot Steel 2 mm (SS2)*, with bending stress correction are shown in Figure 23 (a). A least square fit of the test data is shown in Figure 23 (b). The least square fitted curve is adjusted in order to get a mean value close to zero for variable amplitude loading, see Figure 23 (c). Since the bending stress correction factor is used it is needed to extract two curves that accounts for bending and membrane stress, see Section 3.2.3. The fitted curve is assumed to be representative for the flexible design curve. In previous studies it is concluded that the relation between a stiff and flexible curve is guided by a scaling factor of ∼1.7 [2]. The parameters for the different curves are shown in Table 9. Histograms are presented in Figure 24.

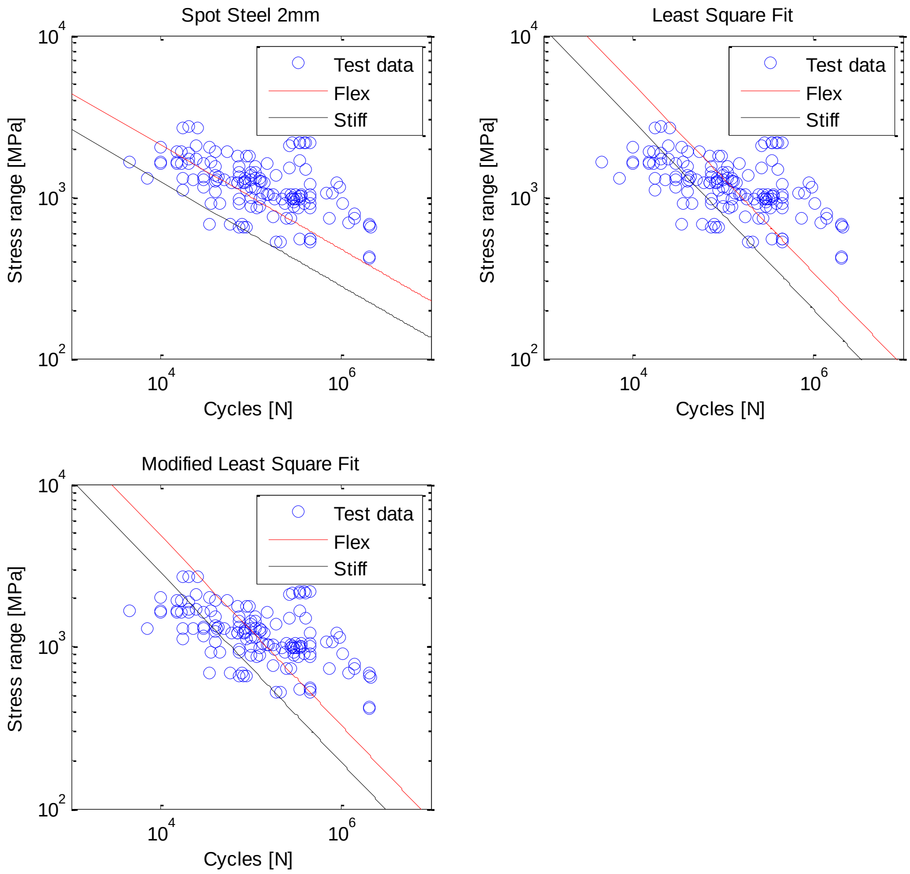

Figure 23. Test scatter and S-N curves for the Seam Weld Module with (a) the Spot Steel 2 mm curve, (b) the least square fit, (c) the modified least square fit.

Table 9. S-N curve parameters for Seam Weld Module, $\Delta\sigma = A \cdot N^b$.

S-N curve	**A**	**b**
LSQ Curve fit, flexible	$1.06 \cdot 10^6$	-0.58
LSQ Curve fit, stiff	$6.25 \cdot 10^5$	-0.58
Modified LSQ Curve fit, flexible	$1.01 \cdot 10^6$	-0.58
Modified LSQ Curve fit, stiff	$5.99 \cdot 10^5$	-0.58
SS2, flexible	$4.01 \cdot 10^4$	-0.32
SS2 , stiff	$2.37 \cdot 10^4$	-0.32

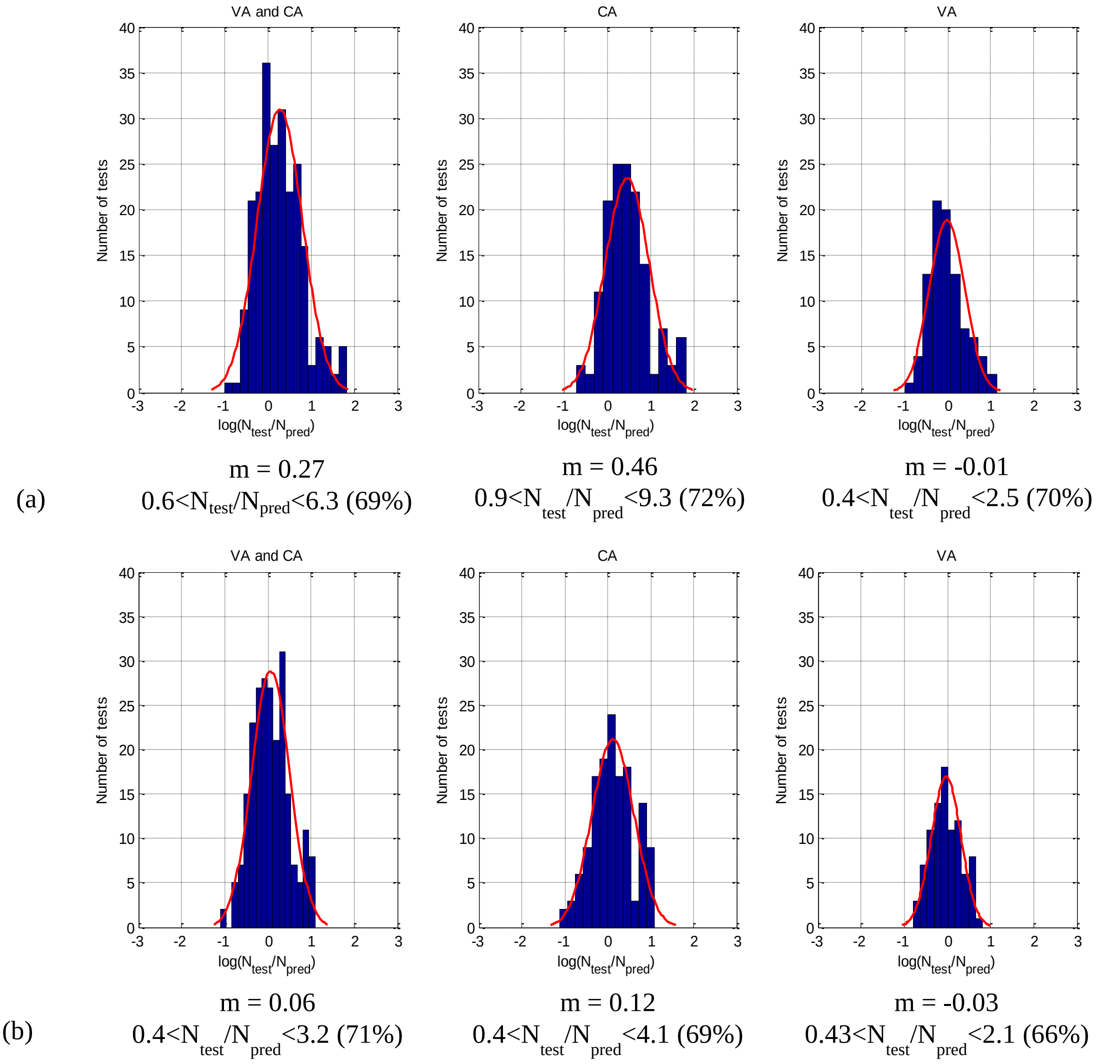

Figure 24. Histograms using the S-N curves for the Seam Weld Module for (a) Spot Steel 2 mm, (b) Modified LSQ.

When comparing the result presented for the SS2 curve and for the modified LSQ fit it is clear that the fitted curve has better prediction intervals for CA and VA loading. The false positives are presented in Table 10. The Seam Weld Module generates a large amount of false positives. When using a fitted S-N curve this number is further increased.

Table 10. False positives using the Seam Weld Module.

Method	**False positives**
Spider SS2	79
Spider LSQ, modified	216

6 Discussion

The anticipated path of this study was to analyse the Spider model, and to change its parameters in order to tune the stiffness of the Spider model. The tuned Spider model was to be used to establish an updated S-N curve. However, when the stiffness of the Spider model was shown to be good using the default settings a new path was set. S-N curves were extracted from the V70 car body tests using two different stress extraction methods. In this way it was possible to learn more about the Spider model and further investigate why the model predicts non-expected fatigue life.

6.1 Stiffness

As mentioned in Chapter 4 the stiffness of the ACM2 model is dependent of the area scale factor of the CHEXA element. With the area scale factor currently used in fatigue analyses at Volvo Cars, the stiffness of the car body is reduced. Figure 25 shows the static torsional stiffness of a car body using the ACM2 model with these parameters. This model also has a general mesh density refined from 10 to 8 mm. It is interesting to see that the stiffness for this model is more or less identical to the stiffness of the car body using the Spider model. This demonstrates that the larger number of false positives in the Spider model does not depend on a weaker car body.

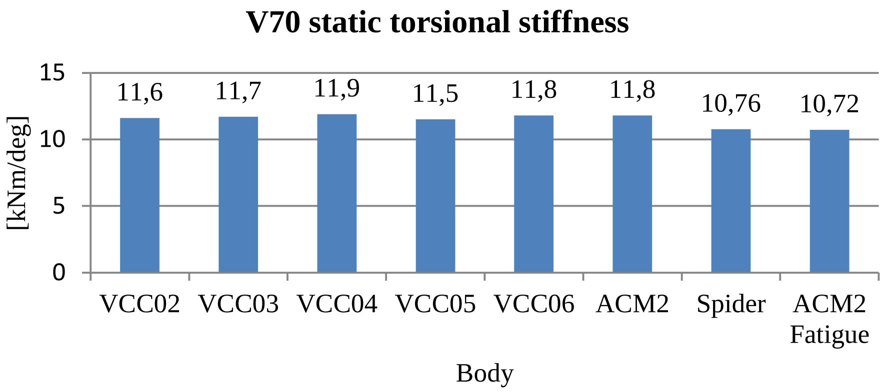

Figure 25. Static torsional stiffness in five car bodies and three FE models.

6.2 Fatigue

In earlier studies of the Spider model at Volvo Cars a significantly reduced spread in the histograms was observed for the Spider model compared to the ACM2 model. In these studies only the spot welds that failed in the physical tests were modelled with the Spider model. In the present study it was possible to calculate the fatigue life of all spot welds using the Spider model and in that way reveal all false positives. Since only one type of car body is studied one cannot draw any general conclusions but this study shows that for the V70 car body, a better prediction interval is associated with a large increase of false positives. Thus, it is not enough to study prediction intervals, false positives also need to be taken into consideration to verify a spot weld model.

In the Spot Weld Module the Spider model shows similar prediction intervals, histograms and false positives as the ACM2 model when using the Spot Sheet Steel S-N curve. This could be expected since similar ways of extracting the stress are used for both methods. This demonstrates that the ACM2 model could be replaced by the

Spider model if using the Spot Weld Module. To make progress of the spot weld modelling technique it would however be more satisfying to use the Seam Weld Module, since the stress around the weld line is found directly in adjacent elements instead of via an analytical solution with assumption of a rigid kernel in a large plate. However, this approach has not been confirmed in this thesis, since a larger number of false positives are generated using this module.

In both Spot Weld and Seam Weld Module the least square fitted S-N curve for the V70 car body differs a lot to the reference curves, which are developed from fatigue coupon tests. In fatigue coupon tests the failure is detected automatically by force or displacement control, while in the V70 fatigue tests the failures are detected by visual inspection. The detecting circumstances are thus much more uncertain in the car body tests. Another explanation to the great difference between the curves could be that there is another type of loading of the spot welds in the car body compared to the fatigue coupon tests. Also, by reducing the slope of the S-N curve the predicted life for high loads is reduced, which better mimics the low cycle behaviour of the spot welds.

6.3 Future recommendations

The V70 model was used in this study since stiffness and fatigue test data was available from the correlation project in 2002. As a consequence of this, a FE model built in the early 2000 was used in simulations. In the context this is an old model and a lot of defects in the model were discovered during the thesis work. FE models built today have a significantly higher quality. A recommendation is to study a contemporary car model to achieve more confident results.

Many poor elements are generated when realising the circular Spider spot welds in a square mesh with element length of 2.5 mm. In order to ensure the quality of the model, bad elements need to be fixed. This process is time consuming. It is desirable that the implementation of the Spider model is improved in order to save time and effort for the user.

The Seam Weld Module predicts many false positives. The reason for this is not found but a future recommendation is to investigate the stress distribution around a spot weld using a fine solid mesh. The stress could then be compared to the stress in the Seam Weld Module.

It is recommended to investigate the use of the hot spot stress approach in fatigue evaluation for spot welds. For seam welds, standards exist of how this should be performed for specific structures. This is widely used in the fatigue design of welded components based on design codes for welded structures [13].

Today an external script is needed to couple the stress from individual nodes to specific spot welds in the Seam Weld Module. It is recommended that this process is included in DesignLife. The 2.5 mm meshed car body is heavy to work with and analyses are time consuming. To make the Spider model easier to work with either a larger mesh size or higher computational power is needed.

Torsion of spot welds was left outside the scoop of this study. One should however consider torsional failure to make the analysis and identification of the Spider model complete. More work is needed to establish relevant fatigue test data and a suitable implementation in FE models.

7 Conclusions

The stiffness of the Spider model was verified for the tested Coach Peel coupons and the V70 car body using the default settings of the Spider model. The hypothesis that non-expected predicted fatigue life should origin from an incorrect stiffness could therefore not be approved.

Two different stress assessment methods were used to estimate the fatigue life of the spot welds in a V70 car body. The results were compared to test results. Both methods gave good prediction intervals but also a large number of false positives. It is therefore concluded that this method of establishing S-N curves is not appropriate.

The S-N curve established in earlier studies at Volvo Cars using the cubic stress assessment shows similar behaviour as the least squares fitted S-N curves. A good prediction interval is achieved but many false positives are also found. This study thus concludes that good histograms and prediction intervals are not enough to verify a spot weld model. The false positives also need to be analysed.

It is seen that using the Spot Weld Module in DesignLife and the analytical stress assessment, the Spider model is equally good as the ACM2 model. If a replacement of the ACM2 model is to be performed at Volvo Cars the Spider model combined with the Spot Weld Module is considered as a suitable alternative until further studies are completed.

8 References

[1] Henrysson, Hans-Fredrik. Fatigue of Spot Welded Joints: Experiments and Life Predictions, ISSN 0346-718X. Chalmers University of Technology, Göteborg, 2001.

[2] Rúnarsson, Àsgeir. Fatigue analysis of spot welded car body structures using shell element structural stresses, M.Sc. Thesis, Report No. 2007:79. Chalmers University of Technology, Göteborg, 2007.

[3] Fritzell, Markus. Fatigue life for different spot weld models. Göteborg, Volvo Car Corporation, Report Dura-CAE-2013-051-01, 2013.

[4] On-Line Reference Manual, Revision date 2013/09/20. Beta CAE Systems SA, Thessaloniki, Greece.

[5] MSC Nastran 2012.2 Documentation, Quick Reference Guide, McNeal Schwendler Corp. Newport Beach, California.

[6] DesignLife Theory Guide. HBM United Kingdom, 2012.

[7] Backhans J, Cedås A. A Finite Element Model of Spot Welds between Non-Congruent Shell Meshes - Calculation of Stress for Fatigue Life Prediction, M.Sc. Thesis, Report No. 2000:13. Chalmers University of Technology, Göteborg, 2000.

[8] Sällström Å. Spot Weld Analysis with Spider Method Guidelines. Report Dura CAE--2007-175-05. Volvo Car Corporation, Göteborg, 2012.

[9] Kang H T, Dong P, Hong J.K. Fatigue analysis of spot welds using a mesh-insensitive structural stress approach. *International Journal of Fatigue* **29**, 1546-1553, 2007.

[10] Taylor D, Zhang Y. Sheet thickness effect of spot welds based on crack propagation, *Engineering Fracture Mechanics* **67**, 55-63. 2007.

[11] Rupp A, Störzel K, Grubisic V. Computer Aided Dimensioning of Spot-Welded Automotive Structures, SAE Paper 950711. SAE International, Warrendale, Pennsylvania, 1995.

[12] Andréasson M, Frodin B. Fatigue Life Prediction of MAG-welded thin sheet structures – theory and experiments, M.Sc. Thesis, Report No. 1997:17. Chalmers University of Technology, Göteborg, 1997.

[13] International Institute of Welding. Recommendations for Fatigue Design of Welded Joints and Components, IIW document IIW-1823-07, June 2008.

[14] Fransson M. Materials Centre, Volvo Car Corporation, Göteborg, 2014.

[15] Klingberg J. Study of Spot Weld Modelling Parameters on Global Static Stiffness and Eigen frequencies, VCC Report 93841-2002-027-02. Göteborg, Volvo Car Corporation, 2003.

[16] Ottosen N, Petersson H. Introduction to the Finite Element Method. Pearson Prentice Hall, Upper Saddle River, New Jersey, 1992.

[17] Fermér M. Main results from the Body Fatigue Correlation Project, VCC Report 93841-2003-076. Göteborg, Volvo Car Corporation, 2003.

Appendix A

Coupon static stiffness test

The tests are load controlled with a given load rate and the stiffness calculation is based on two measurement points. Measurement is taken when the force in the coupon has reached a given level. The complete test matrices can be seen in Table A.1 and A.2.

Table A.1. Static Test Matrix.

Test Parameter	**Lap Shear**	**Coach Peel**
Force Range [kN]	0.1 – 3	0.05 – 0.3
Measure Point 1 [kN]	0.6	0.1
Measure Point 2 [kN]	2.5	0.28
Load Rate 1 [mm/min]	0.01	0.01
Load Rate 2 [mm/min]	0.02	0.02

Table A.2. Dynamic Test Matrix.

Test Parameter	**Lap Shear**	**Coach Peel**
Preload Force [kN]	1.5	0.125
Force Amplitude 1 [kN]	0.65	0.055
Force Amplitude 2 [kN]	1.2	0.1
R_1	0.395	0.389
R_2	0.111	0.111
Frequency Range [Hz]	1 – 100	1 - 100

Appendix B

Distribution of Spider spot welds

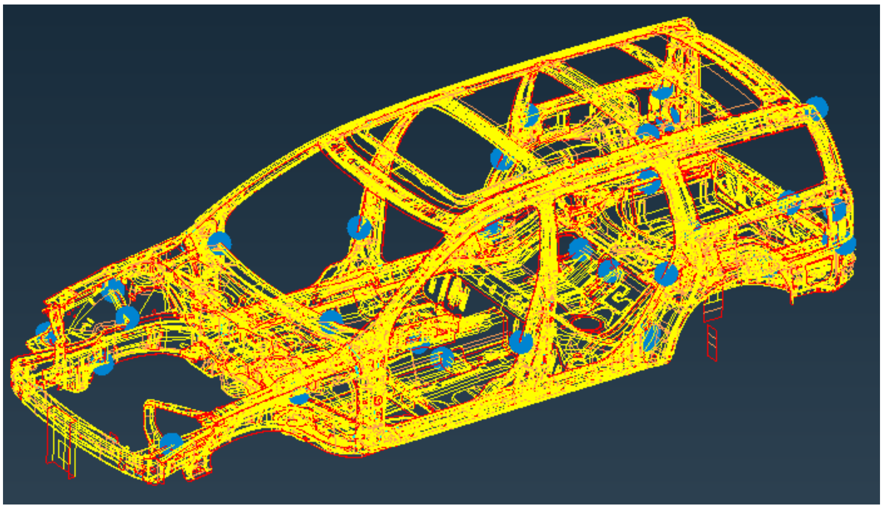

Figure B.1. Moved spot welds.

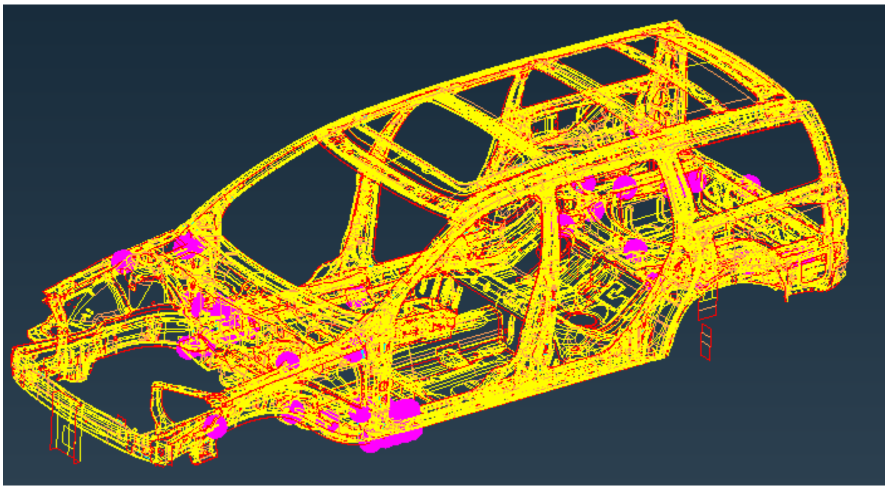

Figure B.2. Connection points without FE-representation.

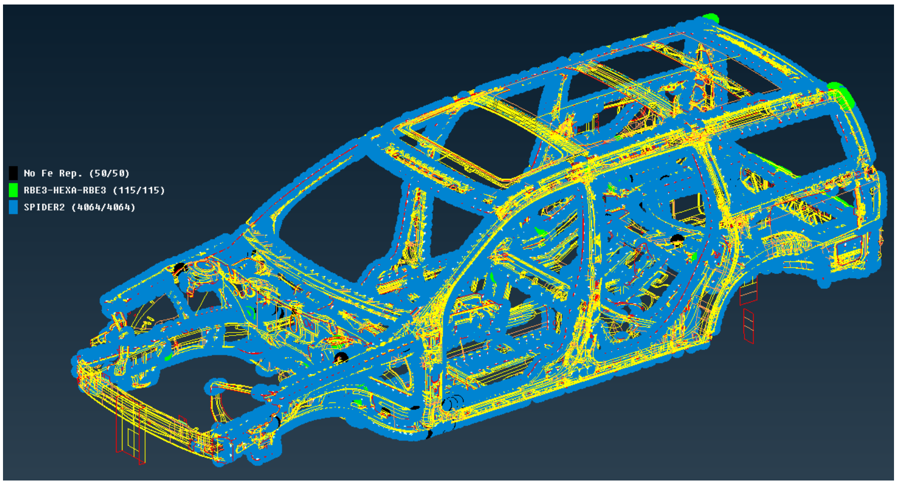

Figure B.3. Distribution of final spot weld representation.

Appendix C

Variable amplitude load signal

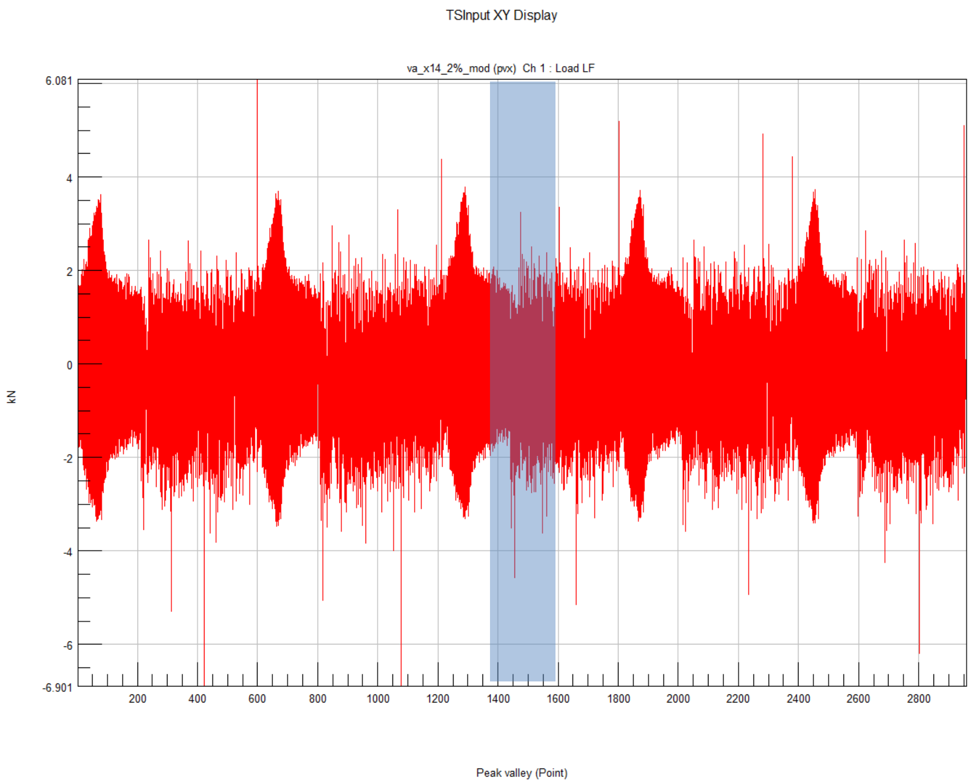

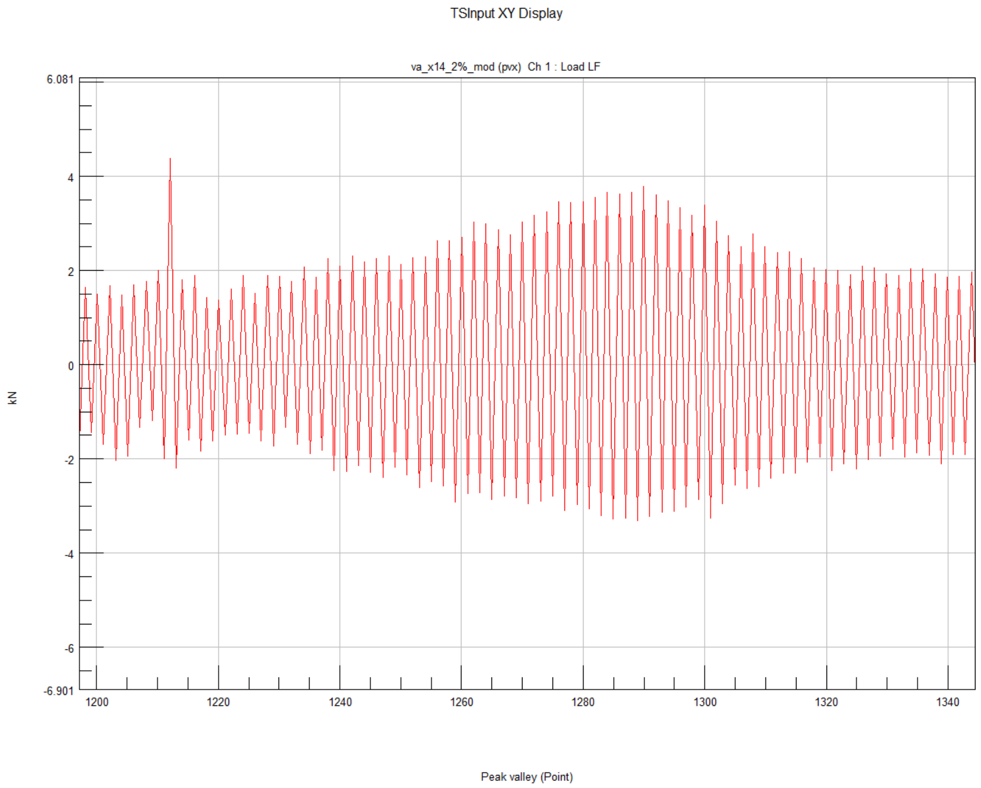

Figure C.1. Load signal with indicated magnification.